

# Exploring the Gap Damper Concept To Control Seismic Isolation Displacement Demands



**H. Zargar & K.L. Ryan**

*University of Nevada, Reno*

**T. Rawlinson & J.D. Marshall**

*Auburn University*

**15 WCEE**  
LISBOA 2012

## **SUMMARY:**

Base isolation systems generally perform well in design-level ground motions to reduce both interstory drift and acceleration demands. During an MCE, however, large displacements in the base level may cause pounding between the structure and perimeter moat wall, which can lead to very high acceleration in the superstructure. A phased passive control device, or “gap damper”, has been conceived to control base isolators displacement during extreme events and prevent violent impacts. This device has no effect on the isolation system performance for earthquakes up to design level. By introducing an appropriate initial gap, the device triggers additional damping during large earthquakes in order to limit displacements. Hysteretic and viscous models are utilized to provide desired additional damping in the device. The effectiveness of the gap damper is demonstrated through simple numerical examples. Schematic illustrations of the proposed physical device being considered for implementation are introduced and discussed.

*Keywords: seismic isolation, MCE event, gap damper, viscous and hysteretic models.*

## **1. INTRODUCTION**

Experimental shake table studies (Fenz and Constantinou 2008, Sato et al. 2011) and physical observation in earthquakes (Stewart et al. 1999) have shown that base isolated systems perform well in design-level earthquakes. Base isolation systems protect the structure by minimizing both acceleration and inter-story drift by lengthening the structure period. Damping in the isolation system can generally be increased to control the isolator displacement demands. However, for typical broadband frequency motions, too much additional damping increases floor accelerations and interstory drifts associated with increased higher mode response (Kelly 1999). Furthermore, during extreme earthquakes such as a Maximum Considered Earthquake (MCE), added damping still may not be sufficient to control the displacement, and pounding or collision of the structure against the outer moat wall may occur (Hall et al. 1995, Makris and Chang 2000, Jangid and Kelly 2001), which transfers a high energy shockwave to the structure. Thus, reliable methods for controlling isolator displacements in extreme ground motions are needed that do not affect the performance of the isolation system in the design earthquake.

To control isolator displacements, we propose a conceptual device that can trigger supplemental damping when a threshold displacement demand is reached. To achieve this, the proposed “gap damper” provides phased behavior by combining a gap element with an energy dissipation device. The damper will not engage at low to medium intensity shaking to preserve the expected performance of the isolation system at this range of earthquake intensity. Various combinations of hysteretic and/or viscous energy dissipation are being considered to identify the best approach to effectively control isolator displacement while preserving superstructure safety by limiting both acceleration and story drifts to acceptable levels. Schematic illustrations of the proposed physical device being considered for implementation are introduced and discussed.

## 2. SYSTEM CONSIDERED

A simple numerical model of an isolated building has been developed to examine the gap damper concept. This system consists of a linear single story shear structure supported atop a bilinear base isolation system. The superstructure roof mass is  $M$  and base mass is  $0.25M$ , representing a multi-story building where the majority of the weight is above the base level. The superstructure has period  $T_s = 0.5$  sec and damping ratio  $\zeta_s = 5\%$ .

### 2.1. Base Isolation Systems Properties

#### 2.1.1. MCE Earthquake

The base isolation system is assumed to have a bilinear force-deformation relation (Fig. 2.1). The properties of the isolator are calibrated for a target secant or effective period  $T_M$  and effective damping ratio  $\xi_M$  corresponding to the isolator displacement  $D_{MCE}$  in an MCE earthquake. A target MCE spectrum with 1.0 second spectral acceleration  $S_{M1} = 1.11g$  and short period spectral acceleration  $S_{MS} = 2.2g$  has been selected.

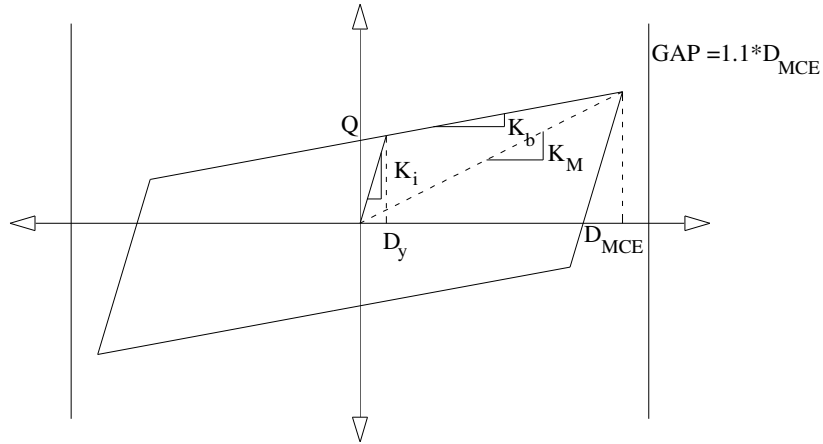


Figure 2.1. Bilinear force- displacement relation of isolation system

The characteristic strength  $Q$  and post-yield stiffness  $K_b$  are computed from  $K_M$ , the effective stiffness corresponding to  $T_M$ , and  $\xi_M$  according to:

$$Q = \frac{K_M \xi_M D_{MCE}}{2(D_{MCE} - D_y)} \quad (2.1)$$

$$K_b = \frac{K_M D_{MCE} - Q}{D_{MCE}} \quad (2.2)$$

where  $D_y$  was assumed to be 1.0 cm. The gap width, or distance to outer moat wall, is assumed to be 10% higher than  $D_{MCE}$  (Fig. 2.1). The primary objective of the gap damper is to limit the base displacement to be less than the gap to avoid impact of the structure with the neighboring moat wall.

#### 2.1.2. Design Earthquake

According to U.S. design procedure, the target design spectrum is  $2/3$  of the MCE spectrum (i.e.  $S_{D1}=2/3 \cdot S_{M1}$  and  $S_{DS}=2/3 \cdot S_{MS}$ ). Since the characteristic strength  $Q$  and post-yield stiffness  $K_b$  are calibrated to the MCE properties as described above, the isolation design period  $T_D$  and damping  $\xi_D$  are determined by iterative calculation (e.g. Ryan and Chopra 2004). For example, in a system with

$T_M=3.0$  sec and  $\xi_M=15\%$ ,  $D_{MCE} = 60$  cm. Using the iterative procedure, the design parameters of this reference isolation system are  $T_D=2.7$  sec,  $\xi_D=23.6\%$  and  $D_D=30$ cm.

## 2.2. Ground Motion Selection and Scaling

A suite of 24 ground motions were selected from PEER NGA database and the SAC Steel Project motions. Two sets of scale factors are utilized for scaling earthquakes. To define the *over-gap scale factors*, selected ground motions are scaled such that when applied to the base isolated system, the isolator displacement exceeds the gap width ( $1.1 \cdot D_{MCE}$ ) by exactly 25%; that is, isolator displacement =  $1.375 \cdot D_{MCE}$ . Scaling to a common starting displacement demand will allow for systematic evaluation of the gap damper ability to reduce the displacement by a large amount (25%). For the design scale factors, ground motions were scaled such that the isolator displacement demand is exactly equal to the design displacement  $D_D$ .

## 3. GAP DAMPER

As discussed before, the gap damper is a passive control device that engages at a threshold displacement to prevent the structure from impacting the perimeter moat wall during extreme seismic events. For this study, the initial gap (threshold displacement) was selected as  $0.6 \cdot D_{MCE}$ , which generally exceeds the design displacement  $D_D$  so that the additional energy dissipation is not active in a design earthquake. The energy dissipation of the gap damper is assumed to be hysteretic damping, viscous damping, or some combination of the two. The parameters of the damper are calibrated to a reference level of energy dissipation  $ED_{PMCE}$ , which is the theoretical energy dissipated by the reference isolation system as it moves from the MCE displacement  $D_{MCE}$  to the over gap displacement  $1.375 \cdot D_{MCE}$  (Fig. 3.1).  $ED_{DAMPER}$  is defined as the energy dissipation of the device as it moves from  $0.6 \cdot D_{MCE}$  (initial gap) to  $D_{MCE}$  (Fig. 3.1). As a starting point for calibration,  $ED_{DAMPER}$  is selected to be equivalent to  $ED_{PMCE}$ ; that is, the energy dissipated by the damper prior to reaching  $D_{MCE}$  is equal to the energy dissipated by the base isolator as it moves from  $D_{MCE}$  to  $1.375 \cdot D_{MCE}$ . In Fig. 3.1, a viscous damping mechanism is assumed for  $ED_{DAMPER}$ .

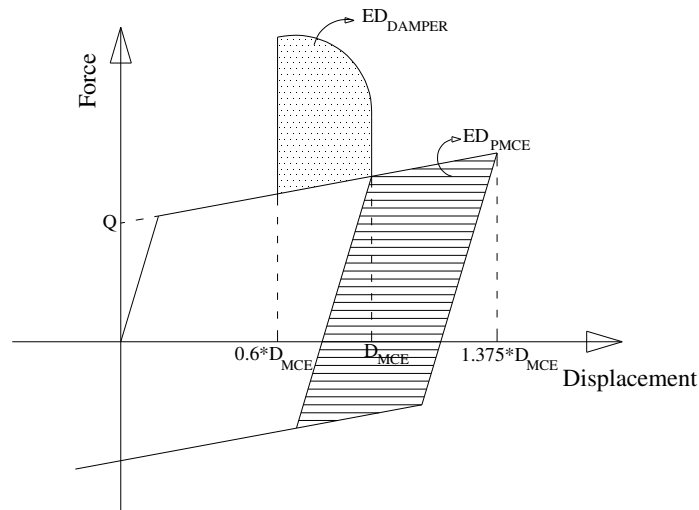


**Figure 3.1.** Finding gap damper properties using equivalent energy dissipation approach

### 3.1. Function of Gap Damper

To show how the gap damper works, the response of a hysteretic gap damper engaged under harmonic load with increasing amplitude, applied to the base level of the system, is illustrated by cycles.

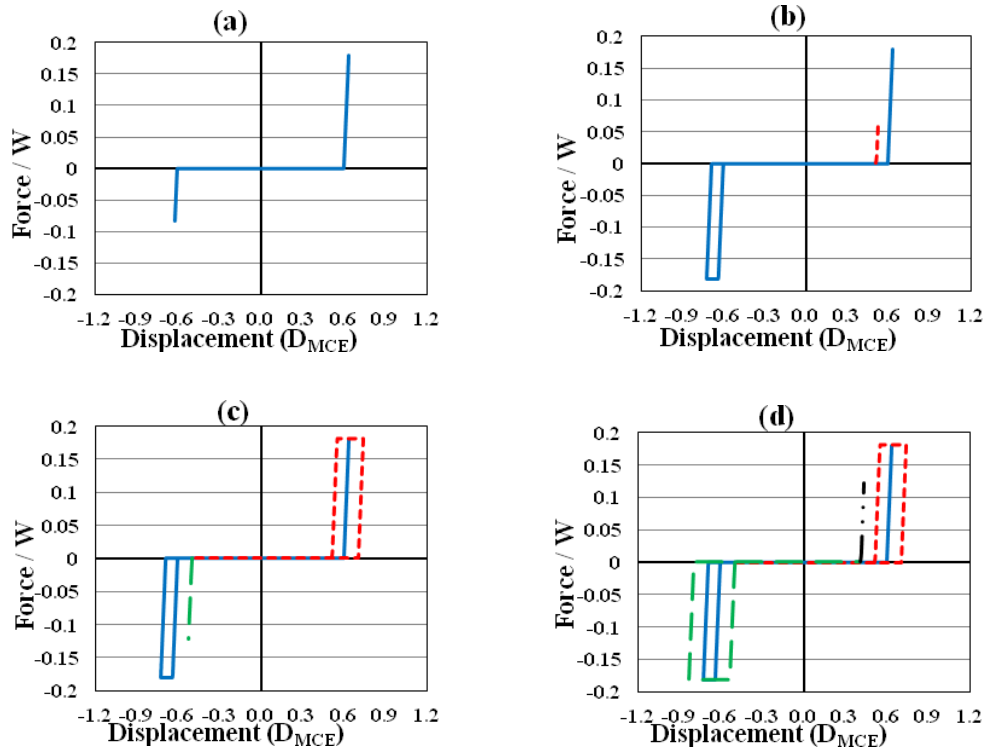


**Figure 3.2.** Cyclic engagement of a hysteretic gap damper under harmonic loading with increasing amplitude

Since the gap damper is hysteretic, the force-deformation is elastic-perfectly plastic. The damper engages initially when the isolator displacement reaches  $0.6 \cdot D_{MCE}$  in either direction. In this example, the gap damper is first activated at a base displacement of  $-0.6 \cdot D_{MCE}$  (Fig. 3.2(a)). The response remains elastic since  $F_{Damp} < F_y$ . The gap damper engages in the other direction at  $0.6 \cdot D_{MCE}$ , but again does not yield. In the next cycle, the device engages again at  $-0.6 \cdot D_{MCE}$  (Fig. 3.2(b)). This time the hysteretic gap damper yields when  $F_{Damp} = F_y$ . After yielding, the response is perfectly-plastic and the displacement increases without any resistance by the damper. In this step, the displacement reaches  $-0.7 \cdot D_{MCE}$  and unloading starts. In the next step, the device engages at  $0.5 \cdot D_{MCE}$  (Fig. 3.2(b)). Physically, the initial gap changes because the device does not re-center upon disengagement, and the total distance between the initial gaps in the two directions remains constant ( $1.2 \cdot D_{MCE}$ ). Thus, since the damper was engaged for a distance  $0.1 \cdot D_{MCE}$ , the initial gaps on the positive and negative side both move accordingly in the same direction. This shifting ability of device increases the energy dissipation compared to a recentering device. Fig. 3.2(c-d) confirm the damper's ability to shift and engage at smaller displacements in both directions as displacement increases. Clearly, the energy dissipation capacity of system increases as the loading amplitude increases.

### 3.2. Gap Damper Models Considered

As mentioned previously, both hysteretic and viscous energy dissipation mechanisms were considered for the gap damper (Fig. 3.3). The hysteretic model is an elastic-perfectly plastic spring, representative of the damping element, in series with a gap element with an initial gap of  $0.6 \cdot D_{MCE}$  (Fig. 3.3(a)). The two gap elements shown in Fig. 3.3(a) each represent device engagement in one direction. Fig. 3.4(a) shows the force-displacement of the combined base isolator and hysteretic gap damper subject to harmonic loading with increasing amplitude.

The viscous gap damper is a linear viscous dashpot in series with a gap element (Fig 3.3(b)), which leads to total force-displacement of the base isolator - gap damper element as shown in Fig 3.4(b). Increased displacement amplitude leads to increased energy dissipation in the viscous gap damper

compared to the hysteretic one. Since the force in the viscous gap damper is proportional to velocity, force increases as displacement amplitude – and hence velocity – increase. In the hysteretic gap damper, however, the damper force is a constant that is independent of displacement or velocity.

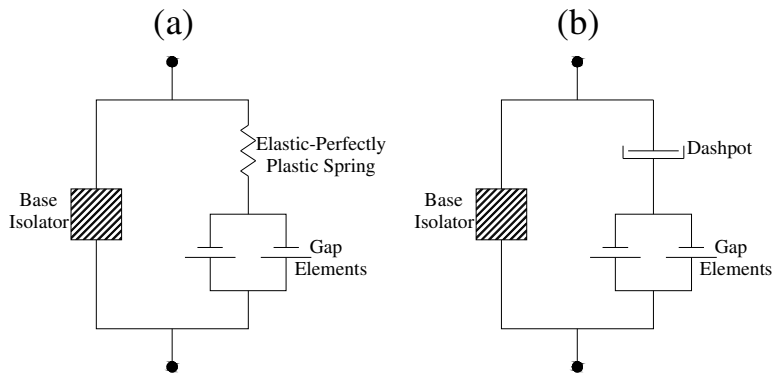


Figure 3.3 Gap damper models: (a) hysteretic model (b) viscous model

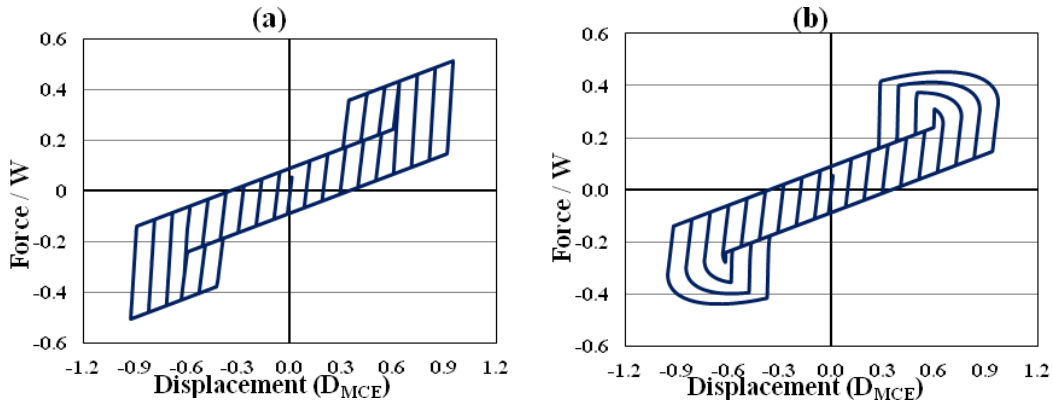
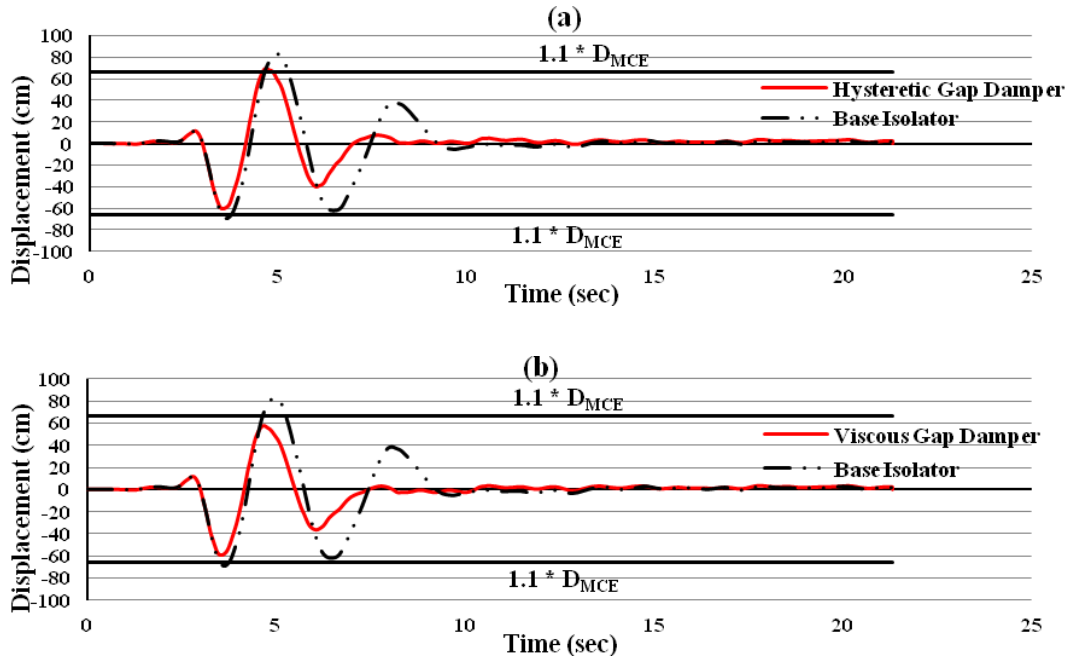


Figure 3.4. Force-displacement history of (a) hysteretic gap damper and (b) viscous gap damper

#### 4. NUMERICAL EXAMPLES

To illustrate the functionality and efficiency of the gap dampers in controlling the system displacement, an analysis of the system with and without a gap damper to the Erizcan-Turkey 1992 ground motion is presented. The displacement histories of the base level for a system with hysteretic and viscous gap dampers are compared in Fig. 4.1, where the displacement of the reference base isolation system ( $T_M=3.0$  sec and  $\xi_M=15\%$ ) without a gap damper is also shown for comparison. The over-gap scale factor was applied to the ground motion. At 5 sec, the base isolator without gap damper reaches the over-gap displacement of 82.5 cm, equal to  $1.375 \cdot D_{MCE}$ . The hysteretic gap damper cannot quite limit the displacement to less than the gap width of 66 cm =  $1.1 \cdot D_{MCE}$ , denoted by black envelope lines in the figures. The maximum base level displacement for this case is 68 cm (Fig. 4.1(a)), which will lead to slight pounding with the outer moat wall. On the other hand, the viscous gap damper limits the displacement to less than the gap for this example (Fig. 4.1(b)). The maximum base level displacement of 60 cm occurs at 3.5 sec, which means the viscous gap damper reduced the peak displacement by 37.5%.

Roof acceleration histories for the examples discussed above are presented in Fig. 4.2. The selected acceleration objective is to limit the roof acceleration to 3 times the median peak roof acceleration



**Figure 4.1.** Base level displacement history of base-isolated system with (a) hysteretic gap damper and (b) viscous gap damper for the Erizcan-Turkey 1992 ground motion

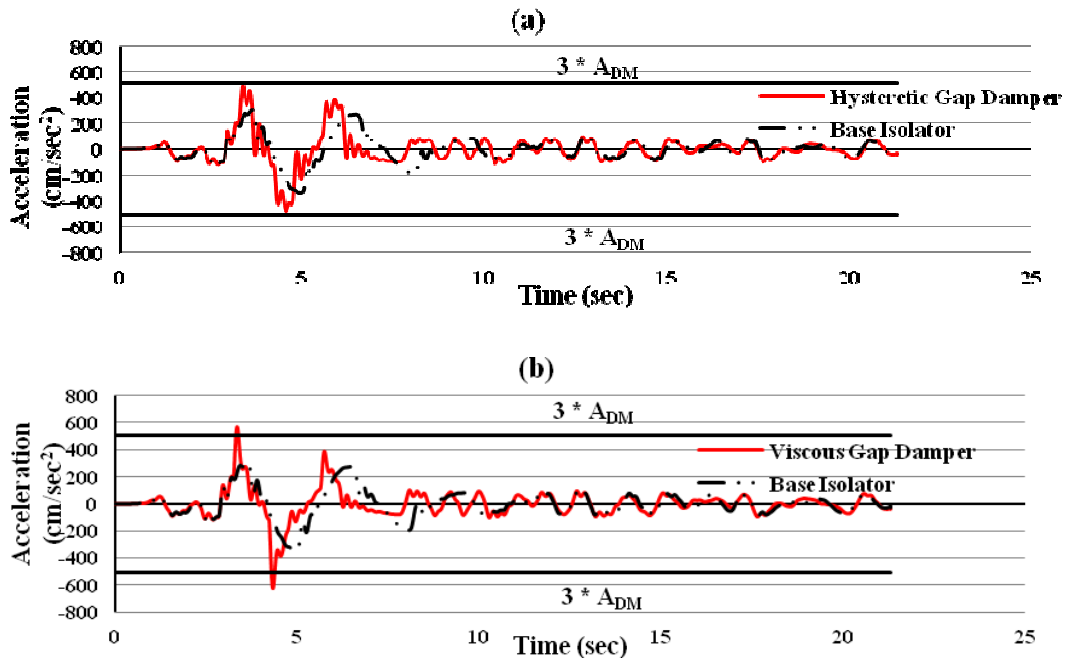


**Figure 4.2.** Roof acceleration history of base-isolated system with (a) hysteretic gap damper and (b) viscous gap damper for the Erizcan-Turkey 1992 ground motion

observed under the design scale factors for the suite of records, denoted  $A_{DM}$ . The effects of pounding between the system and perimeter moat wall were not modeled, so the acceleration history results only show how adding the gap damper would affect the roof acceleration. Figure 4.2 indicates that the hysteretic gap damper meets the acceleration objective while the viscous gap damper does not. In both systems, acceleration spikes occur at approximately 3 sec, 4.5 sec and 6 sec (Fig. 4.2), which

correspond roughly to the time instants when the gap dampers are engaged (Fig. 4.1). Note that the damper first engages at a displacement of -36 cm, but engages at different displacements subsequently due to the shifting of the damper described earlier. The acceleration spikes are a result of the sudden increase in force at the base level when the damper is engaged, as confirmed by force vs. displacement of the system (Fig. 4.3). Shifting is apparent as the gap damper engages at different displacements in each cycle. The viscous gap damper is subject to larger acceleration jumps since, as explained earlier, the force in the viscous damper is larger due to its relation with velocity.

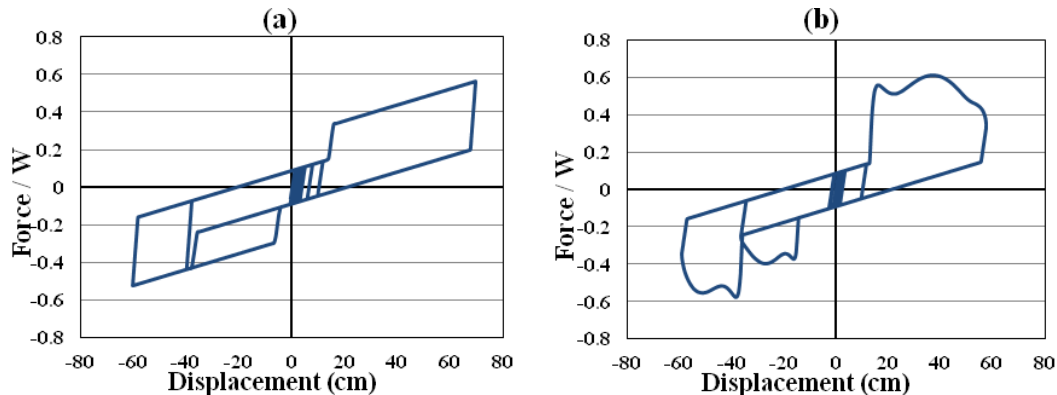


**Figure 4.3.** Force-displacement of the combined base isolation system with (a) hysteretic gap damper and (b) viscous gap damper for the Erizcan-Turkey 1992 ground motion

The examples in this paper have been limited to the basic hysteretic and viscous models for brevity. However, by considering different combinations of viscous and hysteretic models, hybrid models have also been considered. Single phase models engage two energy dissipation devices at the same time, while multi phase models engage different energy dissipation device in different phases with different initial gaps. Our preliminary studies suggest that the relative hysteretic and viscous damping can be optimized in multi phase models to control displacement while minimizing the negative effects on the roof acceleration. The best performing model engages a viscous damper first at a smaller initial gap followed by a hysteretic model at a larger initial gap.

## 5. DEVICE DESIGN AND DEVELOPMENT

Once the most effective method of energy dissipation has been established, the next step is to implement a practical design that can capture the gap damper behavior in addition to meeting other performance objectives. The scaled prototype or possibly multiple prototypes will be fabricated and tested in Auburn University's Structural Research Lab. Using the results of this study, the device will be analyzed and refined before being tested in a scaled structure on the NEES shake table at the University of Nevada Reno.

Several performance objectives were considered in developing a prototype of the gap damper. Bidirectional behavior is a very important aspect of the development of the device. The gap damper device should respond identically in each horizontal direction, regardless of the ground motion direction to ensure protection from the collision with the surrounding wall. This requirement provides the most difficult obstacle to this project as it is challenging to configure a series of gap elements to engage the damping phase bidirectionally. Option #1a (Fig. 5.1) illustrates one possible bidirectional solution. The protruding tube at the top of the figure is attached to the base isolated slab of a building while the concrete pedestals supporting the gap damper device are attached to the ground. When the relative displacement between the isolated slab and the ground reaches the desired activation displacement, the dampers will dissipate energy and effectively limit base displacements and mitigate moat wall collisions.

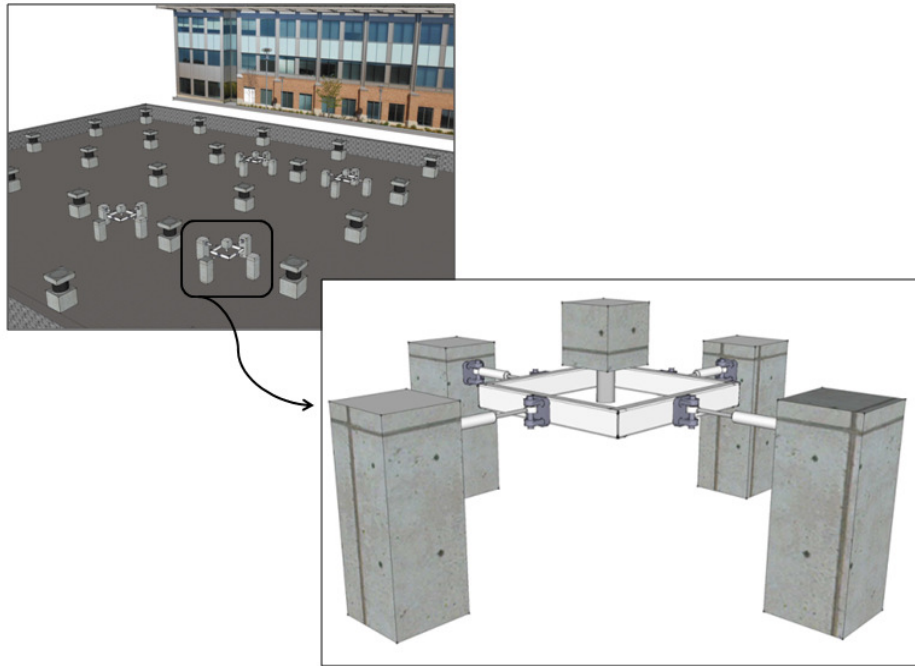


**Figure 5.1.** Option #1a for the gap damper device

Beyond bi-directional behavior, another key issue with the device is reliability. The system is the last line of defense against extreme ground motions before a detrimental collision with the surrounding moat wall; therefore reliable and predictable performance is crucial to the success of this system. Regardless of the ground motion type or direction, the gap damper system must provide reliable and repeatable behavior throughout the duration of the event. Fortunately, viscous dampers are a proven reliable passive device for energy dissipation and the reliability falls solely on the system that utilizes them (Constantinou & Symans 1992). Second, in relation to reliability, the device must be simple and practical for construction in order to minimize mistakes in the field implementation and allow for desired behavior.

To minimize the cost of the system, the dampers should be engaged in both tension and compression. Since the dampers are the most expensive element of the system, each damper should be configured to provide as much energy dissipation as possible for each damper. For example, in Fig 5.1, if the isolated tube moves directly towards one of the dampers and subsequently compresses it, the connectivity of the system with the steel elements allows the opposite damper to act in tension. Therefore, two dampers are activated in a single phase. Options #2 and #3, presented respectively in (Figs. 5.2(b-c)), do not allow for this optimization of damping potential and therefore were dismissed unless an alternative solution for this arrangement could be found. Option #2, similar to Option #1a, provides a protruding tube from a base isolated slab that makes contact with a device attached to the perimeter wall. However, the dampers are only utilized in compression and cannot be recentered. Option #3 provides cables with slack attached from the isolated slab to the dampers, utilizing the dampers in tension only as the slack is tightened and the isolated slab pulls on the device.

Beyond the performance objectives defined previously, other concerns arose as the design concepts were being developed, some specific to a certain concept and others that were general concerns about the system behavior. One issue concerns whether the gap damper device should be located towards the center of the building (Options #1a, #1b, #3, and #4) or the perimeter of the building (Option #2). Although the dampers inherently require minimal maintenance, the inspection of the device may be easier to access in a perimeter device or more efficient if the device is limited to a central location in the middle, depending on the isolation access.

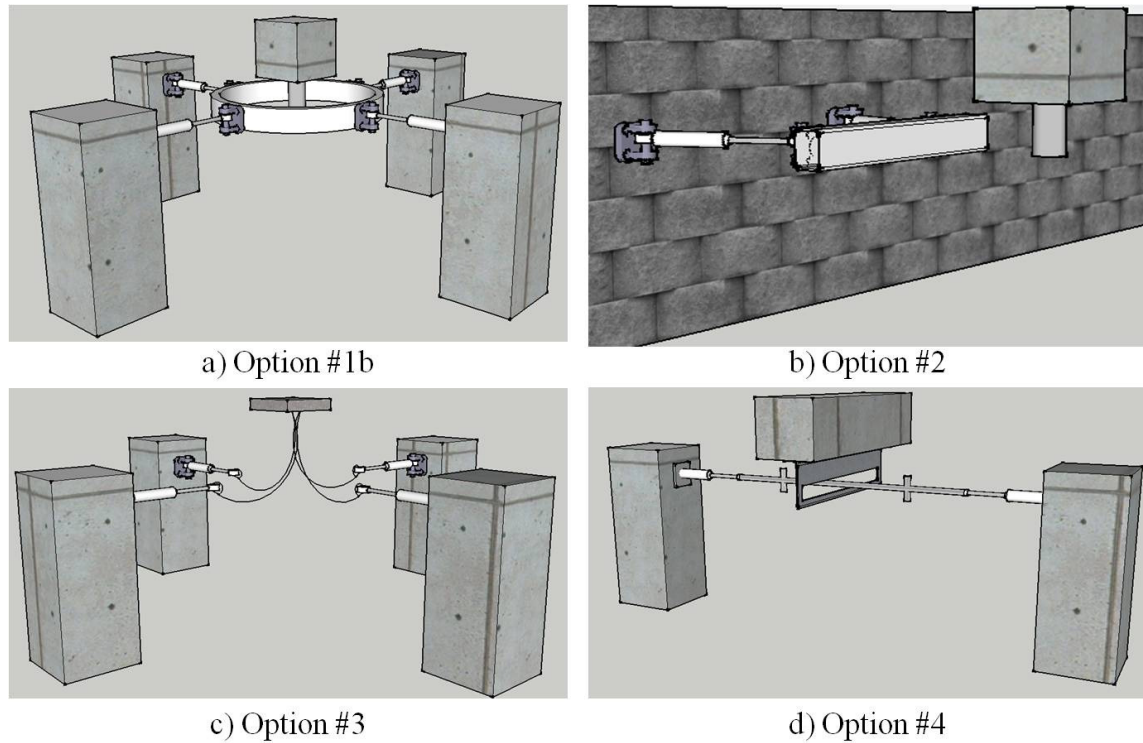


**Figure 5.2** Additional options considered for gap damper configuration

Another concern, especially with Options #1a and #1b is the ability of the dampers to rotate and still displace axially when the applied load is eccentric or completely perpendicular. Given the application of viscous dampers in base-isolated buildings requiring out of plane rotation for bi-directionality, this should not be an issue if detailed correctly. Option #4 provides an alternative solution to this potential issue that would not require the dampers to rotate at all. The slotted angle has a slot that is larger than the max displacement to ensure only axial behavior of the system once the angle reaches the activation pegs in the axial direction of the dampers. The major drawback is that the device is essentially unidirectional so independent devices would be required for each perpendicular direction. Options #1a, #1b, and #4 would require the same number of dampers and supporting pedestals but Option #4 would be needed at two locations rather than one to accomplish the same task.

One of the key elements of the system is the transition from the gap phase to the damping phase, which could have a large effect on the superstructure response upon impact. A two-stage transition may be useful to ease into the phase change. This could be accomplished by adding rubber to the tube connected to the isolation slab in Option #1a and #1b or to the activation pegs in Option #4, pictured in Fig. 5.2(d). Placing the rubber between two tubes would still provide the smooth outside surface for contact but may ease the transition from the gap phase and damper phase. This concept will likely be explored in the preliminary testing of the gap damper device.

Some configurations have the potential to develop large friction forces within the system. For instance in Option #1a, #1b, and #4, if the isolated tube hits the steel element at a sharp angle or the direction of the ground motion changes suddenly, friction forces may be developed in the transverse direction that could potentially modify the behavior of the device. This will also be explored in the preliminary testing to determine if the device can be engaged effectively regardless of the angle of engagement.

Option #1a and Option #1b were grouped together because of obvious similarities. The only difference is the shape of the steel elements, Option #1a, a square, and Option #1b, a circle or

hexagon. When considering motion towards the corner of the building, a circular activation plane may engage too early in relation to the corner of the perimeter wall while a square may activate too late. This is another topic of concern that will be investigated more thoroughly in the research as it proceeds.

Lastly, one other concern with all of the options is the re-centering of the dampers after contact. Preliminary analyses indicate that the residual displacements do not largely affect the performance of the gap damper device. Possibly at a slight cost, a dual acting preload may be manufactured in the damper to re-center after contact. More investigation into this option will be performed in the next phase of the study.

## 6. CONCLUSIONS

The concept of a phased activation device, or gap damper, to control the displacement demands of a base-isolated building in an extreme MCE earthquake without affecting the performance in a design event has been presented. Numerical examples demonstrated that a viscous gap damper can control displacement demands more effectively than a hysteretic gap damper, but at the expense of increased superstructure accelerations. A device engagement mechanism that does not recenter and maintains a constant total gap width between the dampers can provide more energy dissipation for large displacement demands.

Several options for a physical prototype device to provide the requisite gap damping behaviour were presented. The device should engage bidirectionally, and for efficiency engage dampers in forward and reverse cycles (tension and compression). One option for achieving this behavior utilizes dampers attached to grounded concrete pedestals on each side of a square or circular ring. A tab protruding from the isolated base will bump the ring and engage the dampers. The design will be refined and tested at Auburn University and then as part of a system shake table experiment at University of Nevada, Reno.

## ACKNOWLEDGMENT

This material is based on work supported by the National Science Foundation under Grants No. CMMI-1101105 and CMMI-1100922. Any opinions, findings, conclusions, or recommendations expressed in this material are those of the authors and do not necessarily reflect the views of the National Science Foundation.

## REFERENCES

- Constantinou, M.C. and Symans, M.D. (1992). Experimental and analytical investigation of seismic response of structures with supplemental fluid viscous dampers. *Technical Report NCEER-92-0032*, National Center for Earthquake Engineering Research, Buffalo, New York.
- Fenz, DM., Constantinou, MC. (2008). Spherical sliding isolation bearings with adaptive behavior: Experimental verification. *Earthquake Engineering and Structural Dynamics* **37**,185-205.
- Hall, JF., Heaton, TH., Halling, MW., Wald, DJ. (1995). Near-source ground motion and its effects on flexible buildings. *Earthquake Spectra* **11**:4,569-605.
- Jangid, RS. Kelly, JM. (2001). Base isolation for near-fault motions. *Earthquake Engineering and Structural Dynamics* **30**:5,691-707.
- Kelly, JM. (1999). The role of damping in seismic isolation. *Earthquake Engineering and Structural Dynamics* **28**:1,3-20.
- Makris, N., Chang, SP. (2000). Effect of viscous, viscoplastic and friction damping on the response of seismic isolated structures. *Earthquake Engineering and Structural Dynamics* **29**:1,85-107.
- Ryan, KL., Chopra, AK. (2004). Estimation of seismic demands on isolators based on nonlinear analysis. *Journal of Structural Engineering* **130**:3,392-402.
- Sato, E., Furukawa, S., Kakehi, A., Nakashima, M. (2011). Full-scale shaking table test for examination of safety and functionality of base-isolated medical facilities. *Journal of Structural Engineering* **40**,1435-1453.
- Stewart, JP., Conte, JP., Aiken, ID. (1999). Observed behavior of seismically isolated buildings. *Journal of Structural Engineering (ASCE)* **125**:9,955-964.